

## Surface reconstruction using active contour models

Laurent D. Cohen, Eric Bardinet, Nicholas Ayache

► **To cite this version:**

Laurent D. Cohen, Eric Bardinet, Nicholas Ayache. Surface reconstruction using active contour models. [Research Report] RR-1824, INRIA. 1993. inria-00074848

**HAL Id: inria-00074848**

**<https://hal.inria.fr/inria-00074848>**

Submitted on 24 May 2006

**HAL** is a multi-disciplinary open access archive for the deposit and dissemination of scientific research documents, whether they are published or not. The documents may come from teaching and research institutions in France or abroad, or from public or private research centers.

L'archive ouverte pluridisciplinaire **HAL**, est destinée au dépôt et à la diffusion de documents scientifiques de niveau recherche, publiés ou non, émanant des établissements d'enseignement et de recherche français ou étrangers, des laboratoires publics ou privés.

# Rapports de Recherche

N°1824

*Programme 4*

*Robotique, Image et Vision*

## **SURFACE RECONSTRUCTION USING ACTIVE CONTOUR MODELS**

**Laurent COHEN  
Eric BARDINET  
Nicholas AYACHE**

**Fevrier 1993**



**UNITÉ DE RECHERCHE  
INRIA-SOPHIA ANTIPOLIS**

**Institut National  
de Recherche  
en Informatique  
et en Automatique**

**2004 route des Lucioles  
B.P. 93  
06902 Sophia-Antipolis  
France**

# Surface Reconstruction using Active Contour Models

Reconstruction de Surface à l'aide de  
Modèles de Contours Actifs

**Laurent D. COHEN**

CEREMADE, U.R.A. CNRS 749, Université Paris IX - Dauphine  
Place du Marechal de Lattre de Tassigny 75775 Paris CEDEX 16, France.

Email: cohen@bora.inria.fr

**Eric BARDINET and Nicholas AYACHE**

INRIA Centre de Sophia Antipolis

2004, Route des Lucioles BP 93

06902 Sophia Antipolis CEDEX, France.

Email: Eric.Bardinet@sophia.inria.fr Nicholas.Ayache@sophia.inria.fr

February 5, 1993

*Programme 4 : Robotique, Image et vision.*

## Abstract

Variational Methods have been frequently used for surface reconstruction and contour extraction (*snakes*). We present a surface reconstruction method where we assume the surface composed of two regions of different types of smoothness. One region of the surface models a “lake” (constant height region with uphill borders). It is surrounded by the other background region which is reconstructed using classic surface regularization.

The boundary between the two regions, represented by a closed curve is determined with the help of an active contour model. Then the surface is reconstructed by minimizing the energy terms in each region. Minimizing a global energy defined on the couple of unknowns – boundary curve and surface– permits to introduce other forces on the curve. The surface reconstruction and contour extraction tasks are then made together.

We have applied this model for segmenting a synthetic Digital Terrain Model (DTM) image which represents a noisy mountain and lake.

## Résumé

Les Méthodes Variationnelles sont fréquemment utilisées pour la reconstruction de surfaces et l'extraction de contours (*snakes*). Nous présentons une méthode de reconstruction de surface dans laquelle la surface est supposée divisée en deux régions de régularités différentes. L'une de ces régions modélise un “lac” (région d'altitude constante avec des bords qui montent). Elle est entourée par l'autre région qui est reconstruite en utilisant une régularisation de surface classique.

La frontière entre ces deux régions, représentée par une courbe fermée est déterminée à l'aide d'un modèle de contours actifs. Puis la surface est reconstruite en minimisant les termes d'énergie dans chaque région. La minimisation d'une énergie globale définie pour un couple d'inconnues– courbe frontière et surface – permet d'introduire d'autres forces sur la courbe. La reconstruction de surface et l'extraction de contour sont alors effectuées ensemble.

Nous avons appliqué ce modèle pour segmenter une image synthétique de Modèle Numérique de Terrain (MNT) représentant un relief bruité d'un lac entouré de montagne.

## 1 Introduction

Surface reconstruction from noisy data is a fundamental problem which has produced a significant amount of work since many years. Most approaches to surface reconstruction are based on a variational formulation of the problem (see for example [9, 2, 16, 17, 12, 7] and references there). This gives a model of the surface regularity and constraints. Usually the constraints are defined by different types of data and the regularity is the same all over the surface. When regularization is uniform, discontinuities are reduced or removed. Many authors have proposed models to introduce discontinuities in the surface or to smooth the surface adaptively (as in [17, 3, 14, 1]).

We propose a model which corresponds to the particular case when the surface can be segmented into two regions of different regularities. One region models a “lake” surface while the other models the background. The lake region is defined to be horizontal, with uphill borders and its boundary locates on tangent plane discontinuities. The surface function on this region is constant. On the background, the surface is smoothed using a classic first order regularization. As in other models dealing with discontinuities, the problem is that these are unknown. In our model, we assume that the discontinuity set is a closed curve which delimit the “lake” region. Our regularization formulation leads us naturally to locate this curve using an active contour model or “snake” (see [10, 5]). In a first approach, we determine the boundary with a classic snake with a potential adapted to the sought type of borders. We then calculate the surface in each region using the energy minimization.

A second approach consists in considering a global energy defined on the couple of unknowns—surface and boundary. This makes appear a new

force acting on the snake to minimize the surface reconstruction energy.

Our model combines the two problems of surface reconstruction and contour detection using either two separate variational formulations or one global energy to minimize. While we limited ourselves to two connected regions, this could be applied to regions with many connected components using many snakes.

We present results obtained on a synthetic Digital Terrain Model (DTM) representing a lake and mountains. We added noise to the original image to show how the reconstruction behaves. In Fig. 2, we show a 3D plot of these images.

In Sections 2 and 3 we give the necessary background for surface reconstruction and active contour models. We then define our model in Section 4.

## 2 Energy-minimizing Surface Reconstruction

### 2.1 General Approach

Regularization techniques, first introduced as Tikhonov's stabilizers ([18]), have been extensively used in vision research (see for example [9, 16, 7] and references there).

Regularization of the problem of surface reconstruction  $u(x, y)$  given data  $d(x, y)$  is obtained by minimizing the following energy:

$$E(u) = \int \{(u(x, y) - d(x, y))^2\} dx dy + \lambda^2 \int \|\nabla u\|^2 = E_{data}(u) + E_{reg}(u) \quad (1)$$

We minimize simultaneously two terms which correspond to the desired properties:

- a criteria of the faithfulness to the data  $d$ ; and
- a regularizing term containing derivatives of the function.

The solution  $u$  minimizing the energy is a uniformly smoothed version of the data  $d$ . Coefficient  $\lambda$  appears to be a scale factor of the smoothing of the surface. Using a finite difference discretization with the image grid as nodes gives an iterative low pass filter of the image. We show the result of this uniform smoothing on our DTM image in Fig. 4.

## 2.2 Dealing with discontinuities. Mumford & Shah Energy

The regularizing term  $\lambda^2 \int \|\nabla u\|^2 dx dy$  has the same smoothing effect all over the surface. Large variations of elevation in the surface, corresponding to discontinuities between two regions, are attenuated or removed by the smoothing. To avoid this problem, we can either make parameter  $\lambda$  depend on position  $(x, y)$  (as in [17, 8, 15, 3] for example), or introduce discontinuities with penalty (as in [14, 1, 2]).

We will describe the Mumford & Shah Energy-minimizing segmentation and take it as a starting point for a simplified formulation in our particular case. The authors of [14, 2] introduce a penalty term at each point where a discontinuity is detected, instead of its contribution to  $E_{reg}$ . This set of discontinuities is also an unknown of the problem and an argument of the energy. The energy becomes:

$$E(u, B) = \int_R (u - d)^2 + \lambda^2 \int_{R-B} \|\nabla u\|^2 + \alpha l(B) \quad (2)$$

where  $R$  represents the image domain, and  $B$  is a set of boundary points where discontinuities of  $u$  are admitted. The last term  $l(B)$  is the length of this set of contours. The constant  $\alpha$  can be interpreted as a contrast detection factor since a point will choose to be in  $B$  depending of the lower cost either of the gradient contribution in  $E_{reg}$  or paying a penalty  $\alpha$ .

The regularizing effect operates only inside the regions bounded by  $B$ . Thus  $u$  is piecewise regular and can be discontinuous along  $B$ . On

the other hand the penalty term has a regularizing effect on the shape of the boundary  $B$ . This is the advantage of taking a penalty term versus modifying only  $\lambda$  locally.

This energy being non convex, Blake and Zisserman introduced the *graduated non convexity- GNC* (details can be found in [1, 2]). A problem in the GNC approach is that the boundary  $B$  is not always a set of closed curves.

A simplified version of this problem was proposed in [14] for a one dimensional signal and in [13, 11] for images. There, the function  $u$  is supposed piecewise constant and the gradient term is removed. The energy is then:

$$E_c(u, B) = \int_R (u - d)^2 + \alpha l(B) \quad (3)$$

where function  $u$  is constant inside each region defined by boundary  $B$ . When  $B$  is given, the function which minimizes  $E_c$  is easy to find. It is equal on each region to the mean value of the data  $d$  in this region. Then the minimization is made only on  $B$  using a region merging approach. This ensures closed contours but the regularity of these curves is not good enough.

Therefore we propose a model between the two previous approaches using active contours for the boundary. In the next section we give a brief definition of active contour models.

### 3 Active Contour Model

We first recall some definitions and formulate the mathematical problem. For a complete description see [10, 5, 6].

The deformable contour model is a mapping in a space of admissible



deformations  $\mathcal{A}$ :

$$\begin{aligned} & [0, 1] \rightarrow R^2 \\ & s \mapsto v(s) = (x(s), y(s)) \end{aligned}$$

and a functional  $E_{snake}$ . This functional represents the energy of the model which will be minimized and has the following form:

$$\begin{aligned} & E_{snake} : \mathcal{A} \rightarrow R \\ & v \mapsto E_{snake}(v) = \int_0^1 w_1 \|v'(s)\|^2 + w_2 \|v''(s)\|^2 + P(v(s)) ds \end{aligned}$$

where  $v'$  and  $v''$  denote derivatives of  $v$  and where  $P$  is the potential associated to the external forces. The potential is computed as a function of the image data according to the desired goal. If we want the snake to be attracted to edge points, the potential should depend on the gradient of the image. In the following, the space of admissible deformations  $\mathcal{A}$  is restricted by periodic boundary conditions to produce closed curves.

If  $v$  is a local minimum for  $E_{snake}$ , it satisfies the associated Euler-Lagrange equation:

$$\begin{cases} -(w_1 v')' + (w_2 v'')'' + \nabla P(v) = 0 \\ +\text{periodic boundary conditions.} \end{cases} \quad (4)$$

In this formulation each term appears as a force applied to the curve. A solution can be viewed either as realizing the equilibrium of the forces in the equation or reaching the minimum of the energy.

Thus the curve is under control of two types of forces:

- The internal forces (the first two terms) which impose the regularity of the curve. The constants  $w_1$  and  $w_2$  impose the elasticity and rigidity of the curve.
- The image force (the potential term) pushes the curve to the significant lines which correspond to the desired attributes. It is defined by

potential  $P(v) = -\|\nabla I(v)\|^2$ . Here,  $I$  denotes the image. The curve is then attracted by the local minima of the potential, which means the local maxima of the gradient, i.e. edges.

Other forces can be added to impose constraints defined by the user. We will also make use of the inflation force defined in [5]. This inflation force permits to be less demanding of the initialization and to give a simpler initial curve.

After formulating the evolution problem (see [5] using finite differences with time step  $\tau$  and space step  $h$ ) we obtain an iterative scheme of the form

$$(\mathcal{I} + \tau A)v^t = (v^{t-1} + \tau F(v^{t-1})), \quad (5)$$

where  $\mathcal{I}$  denotes the identity matrix.

A correct choice for parameters is guided by numerical analysis considerations. We want the coefficients within the rigidity matrix  $A$  to have similar orders of magnitude. In [5], we obtain good results when the parameters are of the order of  $h^2$  for  $w_1$  and  $h^4$  for  $w_2$ , where  $h$  is the space discretization step.

## 4 Mountain and lake reconstruction

### 4.1 Constraints Definition

Our work is motivated by the application to reconstruction of Digital Terrain Model (DTM) images where we know the presence of a lake. In our examples, we limit ourselves to the case of only one lake but the case of many lake-like regions can be dealt the same way.

A **lake** surface is characterized by the following geometric properties:

1. there is a tangent discontinuity at the boundary;

2. the surface is horizontal;
3. the boundary is at a higher level than the lake.

In such a case, we would like to have a surface function  $u$  obtained by segmentation into two regions:

- the interior of the lake  $L$ , which is a constant region,
- the background  $(R - L)$  which has to be smoothed.

We thus define our solution using an intermediate model between (2) and (3) where we have to find:

- a closed boundary  $B$  separating the lake and background,
- the level of the lake  $u_0$ ; this is the constant value of  $u$  inside the curve,
- the smoothed data  $u$  outside the lake, preserving the constraint that the border is at a higher level than the lake.

## 4.2 Separate Energy Minimizations

We describe in this section a simple approach where we determine first the boundary and then, for this given boundary, calculate  $u$  inside and outside the curve. The three following subsections correspond to items 1 to 3 in the first enumeration of Section 4.1.

### 4.2.1 Boundary Finding

We are looking for the boundary of the lake using an active contour model attracted by the discontinuities of tangent plane (item 1.).

**Active Contour Model.** The boundary  $B$  is supposed smooth and locates on the edge of the lake. It is parameterized by  $v(s) = (x(s), y(s))$ .

We use an active contour model locating a closed curve  $v(s)$  minimizing the energy:

$$v \mapsto E_{snake}(v) = \int_0^1 w_1 \|v'(s)\|^2 + w_2 \|v''(s)\|^2 + P(v(s)) ds$$

The initial curve is manually given inside the lake and then inflated as in [5]. The potential  $P$  has to be chosen such that the minima of  $P$  correspond to lake-like boundary. This boundary is usually called a ramp. A classic step edge detector does not exactly fit this kind of edges and we define the potential accordingly.

**Lake edge Detection.** Classic edge detectors are adapted to find step edges. This corresponds to a gray-level discontinuity, while a lake edge corresponds to a tangent plane discontinuity. Double directional derivative in the direction of the image gradient detects tangent plane discontinuities (see Fig. 1). We thus define the attraction Potential by  $P(v) = -\|\frac{\partial^2 I(v)}{\partial V^2}\|^2$ , where  $V = \nabla I$  is the gradient vector direction. The directional derivative of  $I$  in the direction  $V$  is defined by  $\frac{\partial I}{\partial V} = \frac{V}{\|V\|} \cdot \nabla I$  and the successive derivatives of  $I$  are:

$$\frac{\partial I}{\partial V} = \frac{\nabla I \cdot \nabla I}{\|\nabla I\|} = \|\nabla I\|, \quad \frac{\partial^2 I}{\partial V^2} = \frac{\nabla I \cdot \nabla (\|\nabla I\|)}{\|\nabla I\|} \quad (6)$$

Fig. 3 shows applications of this edge extractor on our image.

#### 4.2.2 Constant Region

Since the lake is perfectly horizontal (item 2.), the inside region is reconstructed by a single elevation level  $u_0$ . As in the case of the energy in (3), we have to calculate only one value  $u_0$  which gives a minimum error on the **inside lake region**  $L$  for:

$$E_{const}(u_0) = \int_L (u_0 - d)^2$$

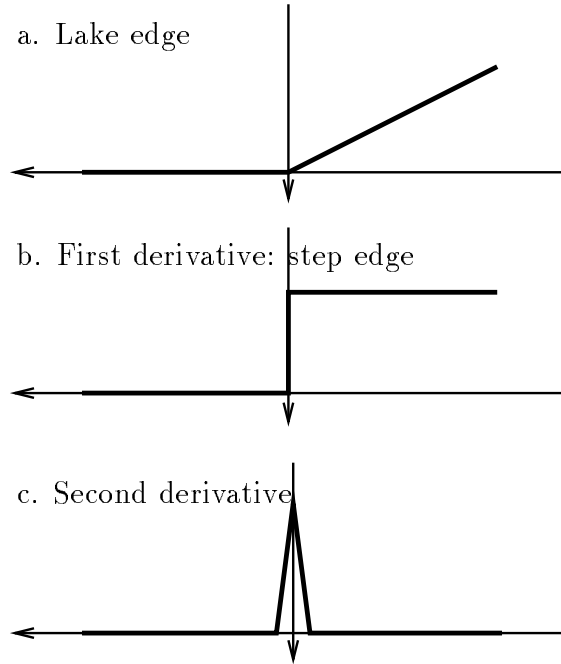


Figure 1: Successive derivations.

It is easy to see that the minimum is reached for the mean value on the region:

$$u_0 = \frac{1}{|L|} \int_L d(x, y) dx dy \text{ where } |L| = \int_L dx dy. \quad (7)$$

#### 4.2.3 Outside Region Reconstruction

In the outside region  $R - L$ , we only apply the “classic” regularization of section 2.1 to which we add a boundary constraint (item 3.). The third item at the beginning of Section 4.1 demands the level at the boundary to be higher than the lake level. This constraint, forcing the borders of the lake-region to go uphill, is added in the energy.

At each point on the boundary, we can define  $n_s$ , the normal to the external surface and  $n_c$ , the normal to the boundary curve (which is in the horizontal plane by definition). The constraint that the level outside the lake is higher than inside can be defined by the dot product

$(n_s, n_c) > 0$ . We impose this constraint by adding to the energy to minimize the following term:

$$E_{border} = \int_{\Gamma} (n_s, n_c)^2 \quad (8)$$

where  $\Gamma$  corresponds to points of the boundary  $B$  determined by the “snake”, such that dot product  $(n_s, n_c)$  is negative.

We can show that using the discretization of the image grid, this dot product can be replaced by  $(u - u_0)$  where  $u$  is the point level outside and  $u_0$  is the level of the lake.

The outside region energy becomes:

$$E_{outside}(u) = \int_{R-L} \{(u(x, y) - d(x, y))^2\} dx dy + \lambda^2 \int_{R-L} \|\nabla u\|^2 + \int_{\Gamma} (u - u_0)^2 \quad (9)$$

In this first approach, we minimize three energy terms one after the other. The first step determines the boundary  $B$  (defined by  $v$ ) and the others calculate the surface  $u$ . Results are shown in Figs. 5 and 6.

$E_{const}$  and  $E_{outside}$  depend clearly in their definition of the detected boundary  $v$  minimizing  $E_{snake}$ . However, this dependence does not appear in the minimization since the boundary is determined in the first step using the active contour model and does change afterwards. Therefore, in the next section, we define a global energy to minimize. This makes the surface terms interact with the active contour model.

### 4.3 Global Energy

We now consider the global energy:

$$\begin{aligned} E_g(u, v) &= E_{snake}(v) + E_{const}(u, v) + E_{outside}(u, v) \\ &= E_{snake}(v) + \int_L (u_0 - d(x, y))^2 dx dy + \\ &\quad \int_{R-L} (u(x, y) - d(x, y))^2 dx dy + \lambda^2 \int_{R-L} \|\nabla u\|^2 + \int_{\Gamma} (u - u_0)^2 \end{aligned} \quad (10)$$

We still minimize the energy successively with respect to the curve  $v$  and the surface  $u$ , but now take into account the dependence on  $v$  of  $E_{const}$  and  $E_{outside}$ . This means that when we determine the boundary curve  $v$ , other forces are added to deform the “snake”.

Assuming we have an estimation of  $u$  everywhere ( using a smoothed version of  $d$  everywhere minimizing the energy of (1)), we minimize the energy with respect to the boundary defined by curve  $v$ . We now have a new global “snake” energy:

$$E_{snake}^g(v) = E_{snake}(v) + \int_{\Gamma}(u - u_0)^2 + \int_L(u_0 - d)^2 dx dy + \int_{R-L}(u - d)^2 dx dy + \lambda^2 \int_{R-L} \|\nabla u\|^2 \quad (11)$$

The first two terms correspond to the integral of some function on the contour. The other terms correspond to the integral of a function either inside or outside this contour. To minimize the energy we have to calculate the differential of each energy term since we deform the curve  $v$  in the direction opposite to the gradient of the energy as seen in Section 3 and [5] for “snakes”.

#### 4.3.1 Curve Integral

This type of term already appears in the “snake” Potential energy:

$$E_{curve}(v) = \int_B f(x, y) dB = \int_0^l f(v(s)) ds \quad (12)$$

The differential is the integral of the gradient of  $f$ :

$$dE_{curve}(v).h = \int_0^l \nabla f(v(s)) h(s) ds \quad (13)$$

The corresponding force applied to the curve is  $F_{curve} = -\nabla f(v(s))$  which is the direction of steepest descent in  $f$  at each point of the curve. This force is already known for the attraction potential  $P$  pushing toward contours.

This type of force also appears in the second term of  $E_{snake}^g$  which is the constraint of  $E_{border} = \int_{\Gamma}(u - u_0)^2 = \int_B((u - u_0)^-)^2$  since  $\Gamma$  is the subset of point of  $B$  such that  $(u - u_0) < 0$  and  $(u - u_0)^-$  is the negative part of  $(u - u_0)$ . Defining  $P_{border}(x, y) = ((u - u_0)^-)^2$ , the corresponding force is  $F_{border} = -\nabla P_{border}(v(s))$ .

#### 4.3.2 Surface Integral

We have to calculate the differential of an energy of the type:

$$E_{surf}(v) = \int_{\Omega} f(x, y) dx dy \quad (14)$$

where  $\Omega$  is the region delimited by the curve  $v$ . Suppose  $h(s)$  is a small deformation of the curve  $v$  and  $\Omega_1$  is the deformed region. The difference of energy is:

$$\begin{aligned} E_{surf}(v + h) - E_{surf}(v) &= \int_{\Omega_1} f(x, y) dx dy - \int_{\Omega} f(x, y) dx dy \quad (15) \\ &= \int_{\Omega_1 - \Omega} f(x, y) dx dy - \int_{\Omega - \Omega_1} f(x, y) dx dy \end{aligned}$$

When  $h$  is small the two regions  $\Omega_1 - \Omega$  and  $\Omega - \Omega_1$  are located around the boundary of  $\Omega$  which we call  $B$ , and it can be shown that the differential is:

$$dE_{surf}(v).h = \int_B f(x, y)(n, h) dB \quad (16)$$

where  $n$  is the external normal to the curve, this means directed outside  $\Omega$ . The corresponding force  $F_{surf} = -f(x, y)n$  can be interpreted as pushing the curve outwards when  $f < 0$  and inwards when  $f > 0$ . In this way it is clear that the integral of  $f$  over  $\Omega$  always decreases.

Back to our problem, the energy involving data  $d$  writes:

$$E_{data} = \int_L (u_0 - d(x, y))^2 dx dy + \int_{R-L} (u(x, y) - d(x, y))^2 dx dy \quad (17)$$



where  $L$  is the inside region of boundary  $B$  and  $R - L$  the outside region. The external normals are opposite in these terms and the differential is:

$$dE_{data}(v).h = \int_B \{(u_0 - d)^2 - (u - d)^2\}(n, h)dB, \quad (18)$$

where  $n$  is the external normal to the lake region  $L$ . The data force which is now added to the other forces applied to the curve is

$$F_{data} = -\{(u_0 - d)^2 - (u - d)^2\}n \quad (19)$$

This force pushes inwards when  $(u_0 - d)^2 > (u - d)^2$ , which is the case if the level  $d$  is far from  $u_0$  and means that we are outside the lake. This helps correcting the boundary of the lake considering the data  $d$  when the contour information is not sufficient. This also permits us to initialize the curve outside the lake. Using a “classic snake” with initial curve outside the lake would not work in our case since there are many edges that would stop the curve and would not allow it to reach the exact boundary. This was the reason why we used previously an initial curve inside the lake. The force  $F_{data}$  avoids this problem and makes the curve go down the “hill” to the lake level.

The other term with the gradient is not used since we already replaced it in the snake energy by the potential  $P$ . We then have a force to attract the curve to high gradient values.

Beginning with a curve which is no more inside the lake, we apply the data force together with the other snake forces to make it stabilize to the new boundary  $B$ . The interior elevation  $u_0$  is computed between iterations since a change of  $B$  makes  $u_0$  different. At the equilibrium, we determine the outside surface also. The result is shown in Fig. 7. We remark that some parts of the boundary went downhill a little too much due to the data force and regularization.

A second example is shown in Figs. 9 and 10. The method is applied to a synthetic image of the same kind but where there is at one border of the lake a staircase like shape. This makes appear step edges close to the contour of the lake and the snake may be stuck to these edges before it reaches the lake (see Fig. 11). But when the global energy is used, the inside surface energy term pushes the snake towards the lake boundary passing through the step edges.

A further study of the parameters and may be their evolution with iterations should improve these results.

## 5 Conclusion

We presented a surface reconstruction method based on a variational formulation. A new aspect of this work is that we assume the surface is composed of two regions of different smoothness. One is planar and horizontal while the other is modeled by a membrane energy. This applies for a Digital Terrain Model which represents a lake surface and the mountainous landscape around. The altitude inside the lake is constant minimizing the error. The surface outside is smoothed using first order regularization.

The main contribution of this work is that we determine the surface together with the boundary of the lake. This boundary is located on discontinuities of tangent plane and the altitude has to increase along the external normal to the border. This contour, defined by a closed regular curve, is found first using an active contour model (“snake”) with external forces adapted to the geometric constraints of our surface and depending also on the surface energy. The surface is calculated easily inside and outside the border using the two surface models.

Although we used only one “snake” and two regions, this could apply to

a surface with many lake-like regions using many “snakes”. As a future extension of this work, we plan to add in the model other differential constraints to include the detection of a “river” like contour. We also wish to apply this method to other types of surface reconstruction like in [4] where differential constraints on the surface normals were used for surface extraction and reconstruction in 3D medical images.

## References

- [1] Andrew Blake and Andrew Zisserman. Some properties of weak continuity constraints and the GNC algorithm. In *Proc. 1986 IEEE Computer Society Conference on Computer Vision and Pattern Recognition*, pages 656–661, Miami, 1986.
- [2] Andrew Blake and Andrew Zisserman. *Visual Reconstruction*. The MIT Press, 1987.
- [3] Isaac Cohen. *Applications des Modèles déformables au traitement d'images médicales*. PhD thesis, Université Paris-Dauphine, 1992.
- [4] Isaac Cohen, Laurent D. Cohen, and Nicholas Ayache. Using deformable surface to segment 3-D images and infer differential structures. In *Proc. Second European Conference on Computer Vision*, pages 648–652, Santa Margherita Ligure, Italy, May 1992.
- [5] Laurent D. Cohen. On active contour models and balloons. *Computer Vision, Graphics, and Image Processing : Image Understanding*, 53(2):211–218, March 1991.
- [6] Laurent D. Cohen and Isaac Cohen. A finite element method applied to new active contour models and 3D reconstruction from cross sections. In *Proc. Third International Conference on Computer Vision*, pages 587–591, Osaka, Japan, December 1990.
- [7] Laurent D. Cohen and Isaac Cohen. Deformable models for 3D medical images using finite elements & balloons. In *Proc. 1992 IEEE Computer Society Conference on Computer Vision and Pattern Recognition*, Champaign, Illinois, June 1992.
- [8] M. Gokmen and C.-C. Li. Edge detection using refined regularization. In *Proc. 1991 IEEE Computer Society Conference on Computer Vision and Pattern Recognition*, Maui, Hawaii, June 1991.
- [9] W.E.L. Grimson. *From Images to Surfaces: A computational study of the Human Early vision system*. The MIT Press, 1981.
- [10] Michael Kass, Andrew Witkin, and Demetri Terzopoulos. Snakes: Active contour models. *International Journal of Computer Vision*, 1:321–331, 1987.
- [11] Georges Koepfler. *Formalisation et Analyse Numérique de la Segmentation d'Images*. PhD thesis, Université Paris IX Dauphine, 1991.
- [12] Simon Lee. *Visual Monitoring of Glaucoma*. PhD thesis, Robotics Research Group, Department of Engineering Science, University of Oxford, 1991.
- [13] Jean-Michel Morel and Sergio Solimini. Segmentation d'images par méthode variationnelle: une preuve constructive d'existence. *Comptes Rendus de l'Académie des Sciences*, 1988.

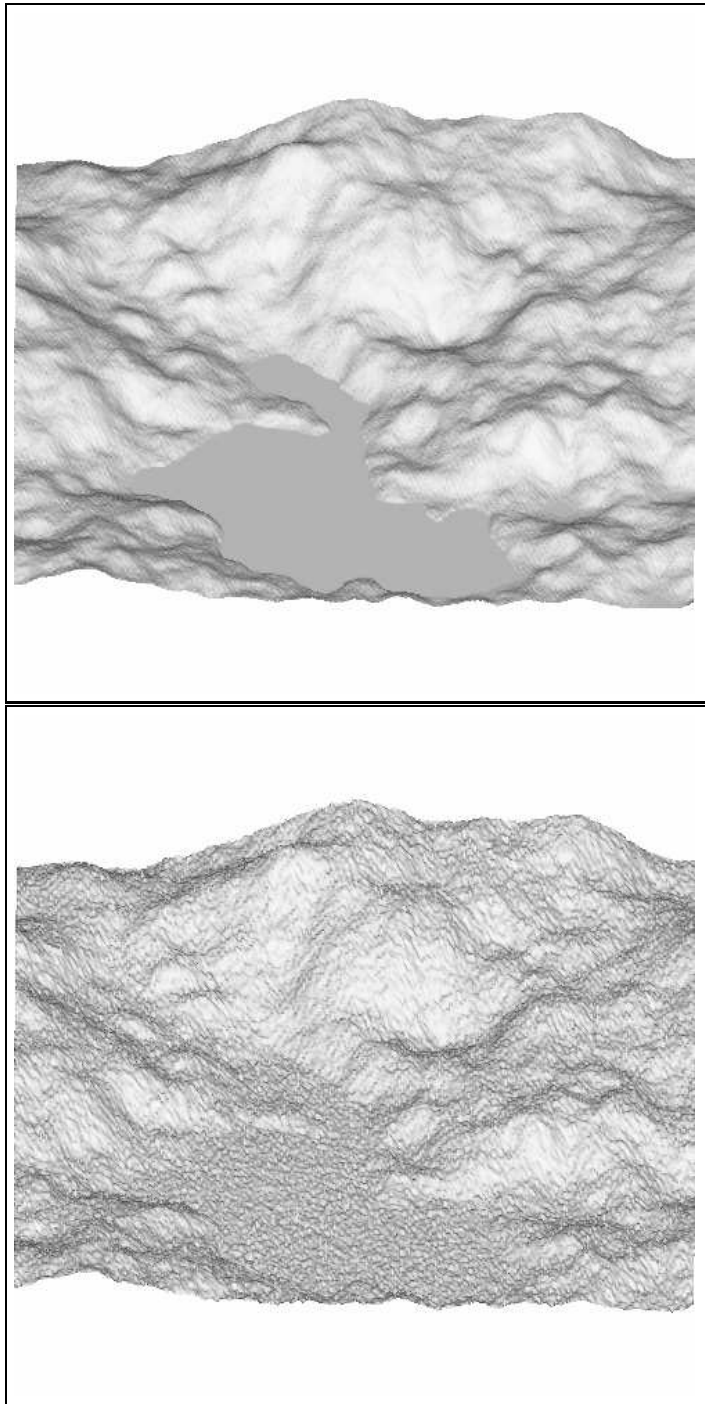


Figure 2: Digital Terrain Model (DTM) Plot; original and noisy images.

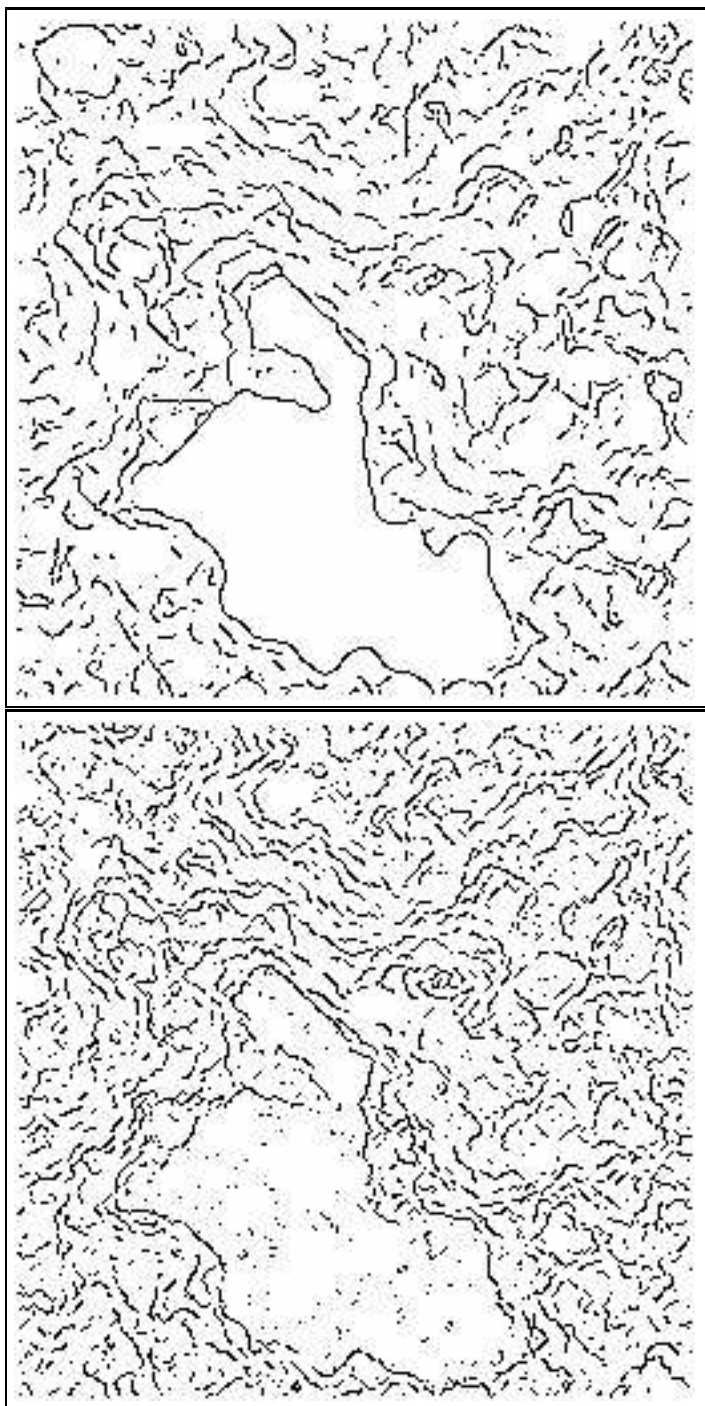


Figure 3: Lake edge extraction on the original and noisy image.

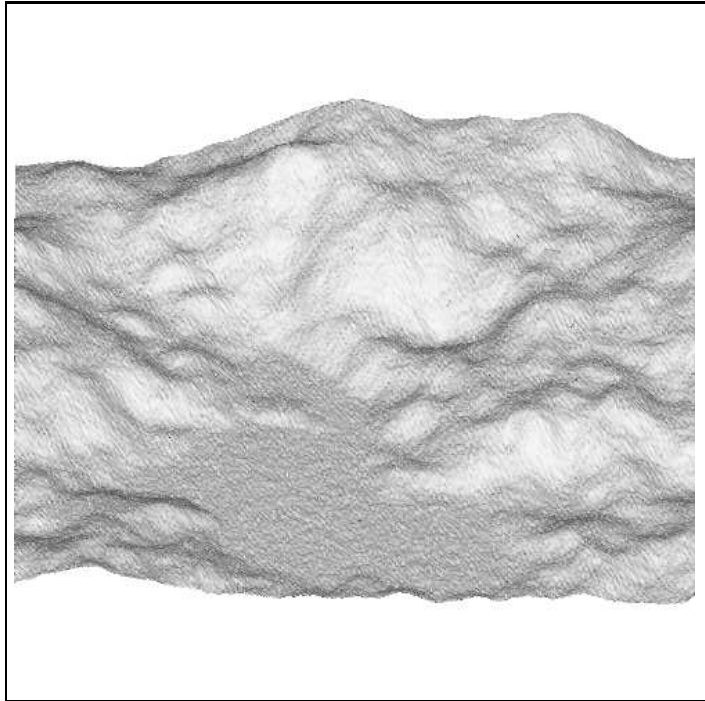


Figure 4: classic regularization.

- [14] D. Mumford and J. Shah. Boundary detection by minimizing functionals. In *Proceedings of Computer Vision and Pattern Recognition*, San Francisco, June 1985.
- [15] S. Sinha and B. Schunk. Surface approximation using weighted splines. In *Proc. 1991 IEEE Computer Society Conference on Computer Vision and Pattern Recognition*, Maui, Hawaii, June 1991.
- [16] Demetri Terzopoulos. Regularisation of inverse visual problems involving discontinuities. *IEEE Transactions on Pattern Analysis and Machine Intelligence*, PAMI-8(4):413–424, July 1986.
- [17] Demetri Terzopoulos. The computation of visible-surface representations. *IEEE Transactions on Pattern Analysis and Machine Intelligence*, PAMI-10(4):417–438, July 1988.
- [18] A.N. Tikhonov and V.Y. Arsenin. *Solutions of ill-posed problems*. Winston and sons, 1977.

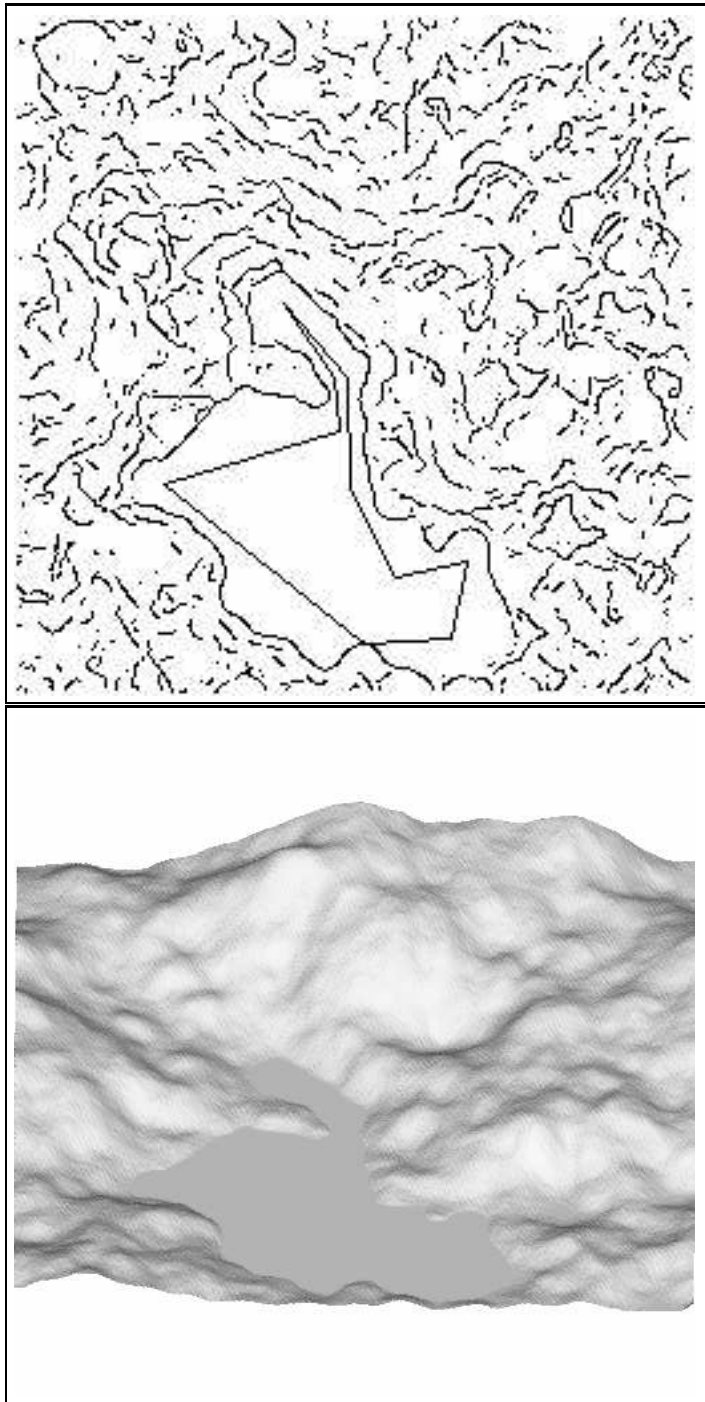


Figure 5: Contour Initialization and original MNT reconstruction with constraints.



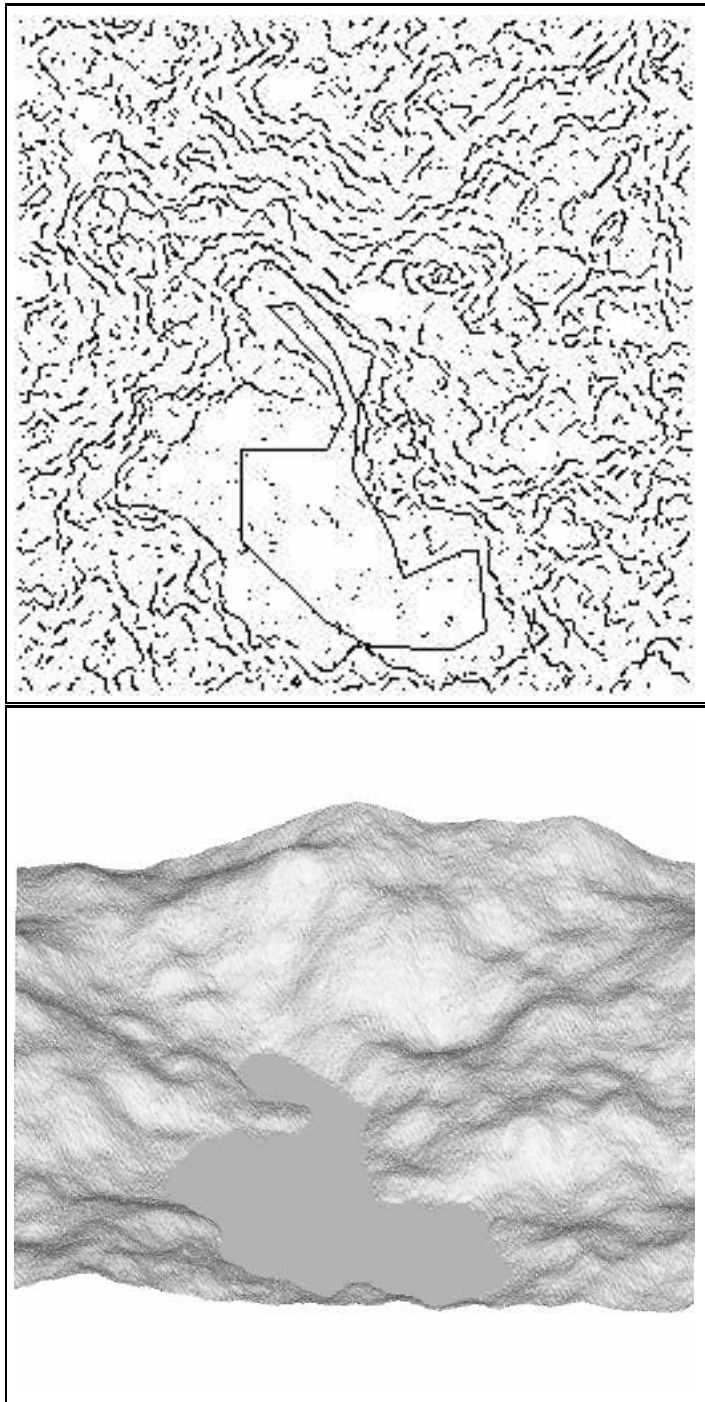


Figure 6: Contour Initialization and noisy MNT reconstruction with constraints.

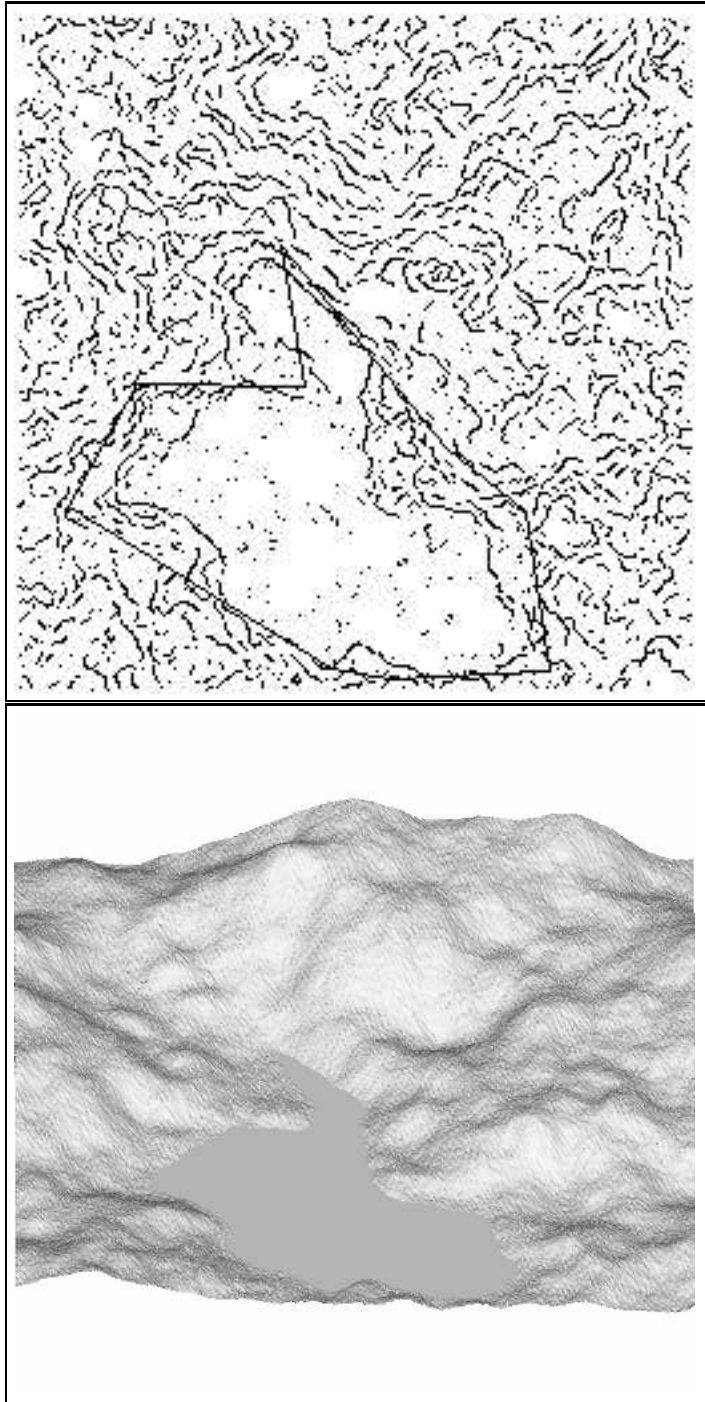


Figure 7: Contour Initialization and noisy MNT reconstruction with global energy.

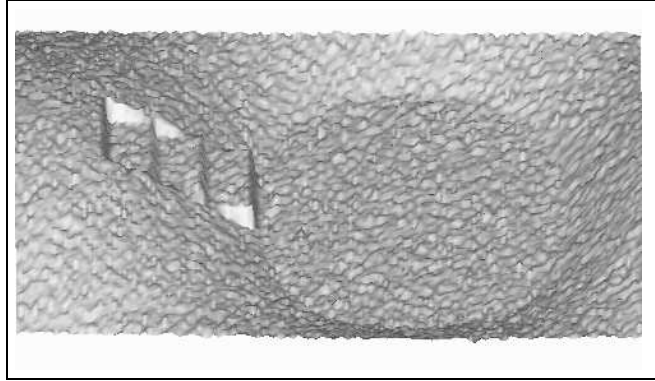


Figure 8: Original noisy MNT.

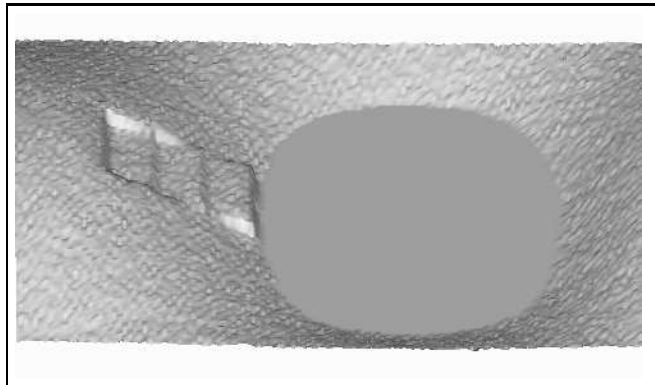


Figure 9: Reconstruction of noisy MNT with global energy.

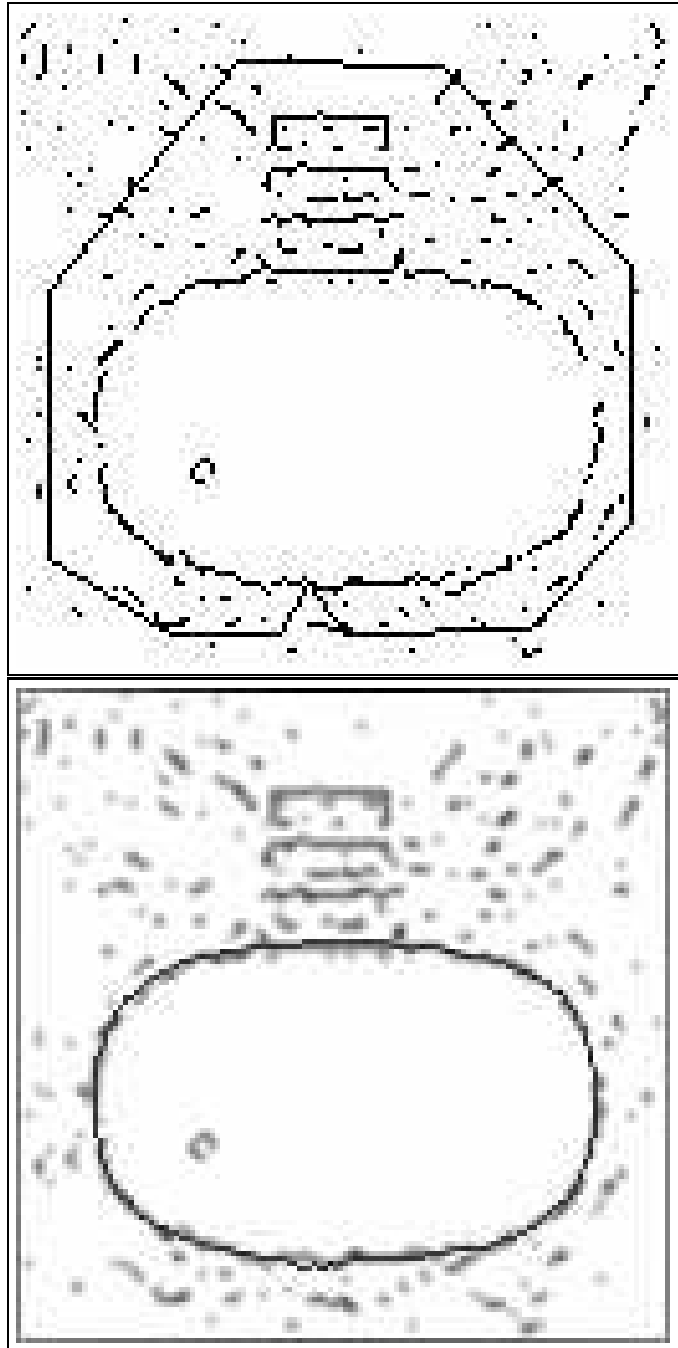


Figure 10: Contour Initialization and result on noisy MNT with global energy.

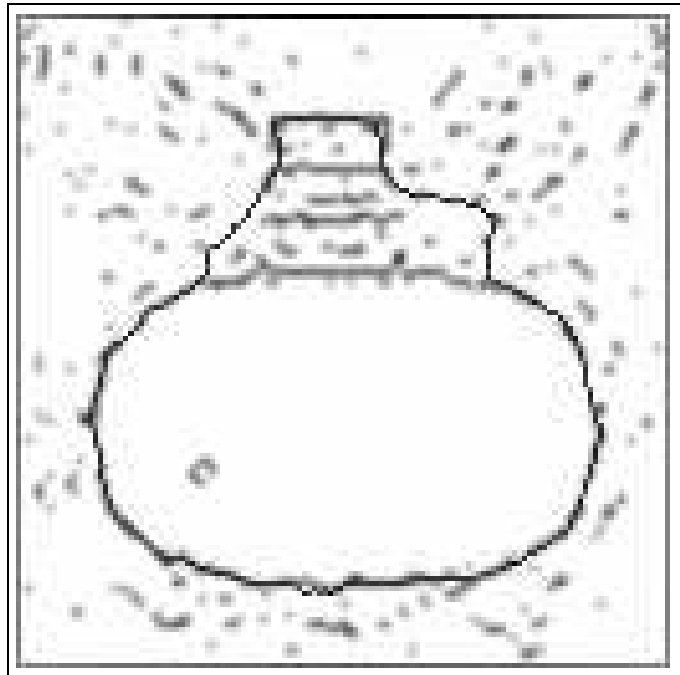


Figure 11: Contour stopped by the first edges encountered when using a classic snake. the initialization is the same as in the previous figure.